This article was downloaded by:
On: *25 January 2011*
Access details: *Access Details: Free Access*
Publisher *Taylor & Francis*
Informa Ltd Registered in England and Wales Registered Number: 1072954 Registered office: Mortimer House, 37-41 Mortimer Street, London W1T 3JH, UK

Separation Science and Technology

Publication details, including instructions for authors and subscription information:
http://www.informaworld.com/smpp/title~content=t713708471

Separation of Proteins via pH Parametric Pumping

H. T. Chen[a]; U. Pancharoen[a]; W. T. Yang[a]; C. O. Kerobo[a]; R. J. Parisi[a]
[a] DEPARTMENT OF CHEMICAL ENGINEERING, NEW JERSEY INSTITUTE OF TECHNOLOGY NEWARK, NEW JERSEY

To cite this Article Chen, H. T. , Pancharoen, U. , Yang, W. T. , Kerobo, C. O. and Parisi, R. J.(1980) 'Separation of Proteins via pH Parametric Pumping', Separation Science and Technology, 15: 6, 1377 — 1391

To link to this Article: DOI: 10.1080/01496398008068511

URL: http://dx.doi.org/10.1080/01496398008068511

PLEASE SCROLL DOWN FOR ARTICLE

Full terms and conditions of use: http://www.informaworld.com/terms-and-conditions-of-access.pdf

This article may be used for research, teaching and private study purposes. Any substantial or systematic reproduction, re-distribution, re-selling, loan or sub-licensing, systematic supply or distribution in any form to anyone is expressly forbidden.

The publisher does not give any warranty express or implied or make any representation that the contents will be complete or accurate or up to date. The accuracy of any instructions, formulae and drug doses should be independently verified with primary sources. The publisher shall not be liable for any loss, actions, claims, proceedings, demand or costs or damages whatsoever or howsoever caused arising directly or indirectly in connection with or arising out of the use of this material.

SEPARATION SCIENCE AND TECHNOLOGY, 15(6), pp. 1377–1391, 1980

Separation of Proteins via pH Parametric Pumping

H. T. CHEN,* U. PANCHAROEN, W. T. YANG,
C. O. KEROBO, and R. J. PARISI

DEPARTMENT OF CHEMICAL ENGINEERING
NEW JERSEY INSTITUTE OF TECHNOLOGY
NEWARK, NEW JERSEY 07102

Abstract

An equilibrium theory is used to study pH parametric pumps. Simple graphical procedures for predicting the separation are presented. It is shown that a parapump with a series of columns packed alternately with cation and anion exchangers is capable of yielding very high separation factors. Experimental results are in qualitative agreement with theory.

INTRODUCTION

Parametric pumping is a separation process which involves reciprocating flow of the mixture to be separated through a fixed bed and, simultaneously, synchronous cyclic variation of an intensive variable, such as gas pressure, solution temperature, or solution pH. Applications of parametric pumping involving the separation of valuable materials such as proteins would be very attractive and profitable to investigate.

Many experimental and theoretical studies have been carried out for the separations by thermal and heatless (or pressure cycling) parametric pumping. By contrast, very little work has been done on pH parametric pumping. Included are the studies of Sabadell and Sweed (*6*), Shaffer and Hamrin (*7*), and Chen et al. (*1*, *2*).

In this paper we investigate various versions of pH-driven parametric pumps. We apply a simple equilibrium theory (*3–5*) to predict the protein separation. Also, some experimental results are presented.

*To whom correspondence should be addressed.

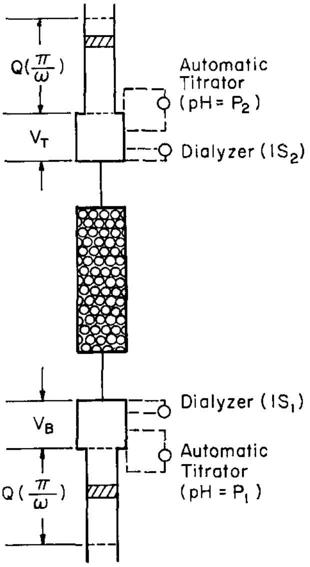

FIG. 1. Column diagram for pH parametric pumping.

ONE-COLUMN PARAMETRIC PUMPING SYSTEM

The first system we will consider is shown in Fig. 1. It consists of a column packed with an ion exchanger (cation or anion) and reservoirs attached to each end. The pump has dead volumes V_T and V_B for the top and bottom reservoirs, respectively. Initially, the mixture to be separated fills the column voids, the top reservoir, and the bottom dead volume. The top reservoir is maintained at a low pH level (P_2) by an automatic titrator while a second titrator is used to keep the bottom reservoir at a high pH level (P_1). The buffer ionic strengths for solutions in both top and bottom reservoirs are kept at IS_2 and IS_1, respectively, by means of two hollow fiber dialyzers manufactured by Amicon.

Two constant pH fields (P_1 and P_2) are imposed periodically on the system. During the first half-cycle, the fluid with pH = P_2 in the top reservoir is pumped into the top of the column. At the same time, solution that emerges from the column fills the bottom reservoir. On the next half-cycle, the solution with pH = P_1 in the bottom reservoir flows back to the column. At the end of this half-cycle, the top reservoir is filled with the solution that comes forth from the top of the column, and one cycle is completed. This procedure is repeated in each of the succeeding cycles until the desired number of cycles is obtained.

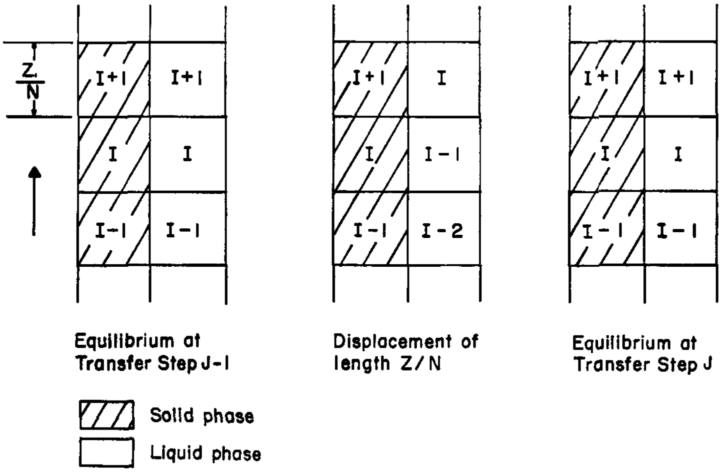

FIG. 2. Schematic for equilibrium plug flow model.

EQUILIBRIUM PLUG FLOW MODEL

We will deduce the characteristics of the pH parametric pump described above via a simple discrete transfer equilibrium stage model. Let us assume that the adsorbent bed is divided into N equal segments or cells (stages) of length Z/N, where Z is the length of the pump column. Each stage is represented as (I, J), where I is the stage number and J is the transfer step (Fig. 2). The system is initially in equilibrium at $J - 1$, and each cell has uniform concentrations in both fluid and solid phases. In the transfer step each fluid section is displaced exactly one step ahead. Thus the fluid $y(I, J - 1)$ originally opposite the solid section I is now opposite $I + 1$. After the transfer step the phase equilibrium is immediately reestablished and the next transfer step J begins.

The mass balance for each component at I and J is

$$Vy(I - 1, J - 1) + \bar{V}x(I, J - 1) = Vy(I, J) + \bar{V}x(I, J) \tag{1}$$

where V and $\bar{V}$ are the volumes of the fluid and the solid phases per stage, respectively, and will be assumed to be constant. Furthermore, we will make the following assumptions:

(a) The solute will be distributed between the solid and fluid phases according to a linear form,

$$x = ky \tag{2}$$

where k is pH-dependent only.

(b) Hydrogen ion does not exchange for the exchanger's counterion, and therefore there is no lag of pH wave velocity behind the linear liquid velocity.

Proteins carry both negatively and positively charged groups and can be bound to both anion and cation exchangers. Their net charge is dependent on pH. At low pH the net charge is positive; at high pH it is negative. At the point of zero net charge, the isoelectric point, the substances are not bound to any type of ion exchanger.

Suppose we are concerned with the separation of a Protein A from a mixture or solution, and this protein has the isoelectric point I_A and $P_2 < I_A < P_1$. Thus A will bear a negative charge at P_1 and a positive charge at P_2, whereupon A will be taken up by a suitable cationic exchanger, R^- (with the counterion S^+) at P_2 and released at P_1:

$$R^-S^+ + A^+ \rightarrow R^-A^+ + S^+, \qquad \text{at } P_2$$
$$R^-A^+ + S^+ \rightarrow R^-S^+ + A^-, \qquad \text{at } P_1$$

Therefore, a parametric pump operating with levels of P_1 and P_2 should be capable of removing the Solute A from the low pH end of the column and concentrating it at the high pH end. A reversed effect will occur if an anion exchanger is selected.

Concentration transients calculated by means of Eqs. (1) and (2) are shown in Fig. 3. The ordinate is the average reservoir concentration divided by the initial liquid-phase concentrations. As long as $\alpha = 1$, the steady-state concentrations in both top and bottom reservoirs are independent of N chosen. α is defined as the quotient of the reservoir displacement and the column void volume (i.e., number of transfer steps/number of stages). Note that when $\alpha = 1$, $N = Q(\pi/\omega)/V$.

GRAPHICAL SOLUTION FOR ONE-COLUMN SYSTEM

The approach presented here starts from the model of Grevillot and Tondeur (*3*). However, they are concerned with the direct mode of thermal parametric pumping, and we extend it to the recuperative mode of pH parametric pumping. Also, the development is based on $N = 1$ and $\alpha = 1$. As stated before, when $\alpha = 1$, the steady-state separation is independent of the stages (N) chosen.

The pump consists of a column packed with cation exchanger and reservoirs attached to each end. The pH values of the top and bottom reservoirs are maintained at given levels P_2 (= 6) and P_1 (= 8), respectively.

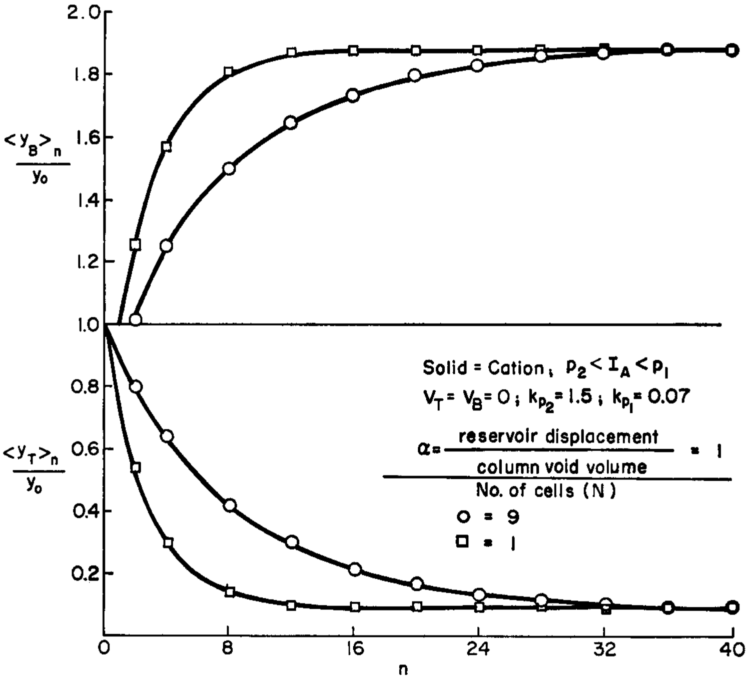

FIG. 3. Effect of N on concentration transients.

As shown in Fig. 4, the operation begins with the column filled with the mixture of concentration y_0, everywhere at equilibrium with the solid. The initial pH in the column is high (or $P_1 = 8$). Also, there is fluid of the same initial concentration in the top reservoir. The first fluid motion is downward, and $V_T = V_B = 0$. Let x and y be the concentration of A in the solid and fluid phases, respectively. Using Eq. (2), we draw two equilibrium lines (with slopes equal to k_{p_1} and k_{p_2}) on an x–y diagram. The initial concentration in the column (y_0; x_0) is represented by the point y_0. One cycle of the operation includes four steps, and the effect of the operation for the first cycle is as follows:

(a) Transfer down: The fluid in *TR* (top reservoir) is transferred to the column, and the fluid in the column is transferred to *BR* (bottom reservoir). Therefore, the bottom reservoir concentration for the first cycle is y_0.

(b) Equilibration at P_2: The column pH is changed from P_1 to P_2. The two phases are then allowed to equilibrate at P_2. This leads to a new composition in the column (y_{T1}; x_{T1}), represented by the

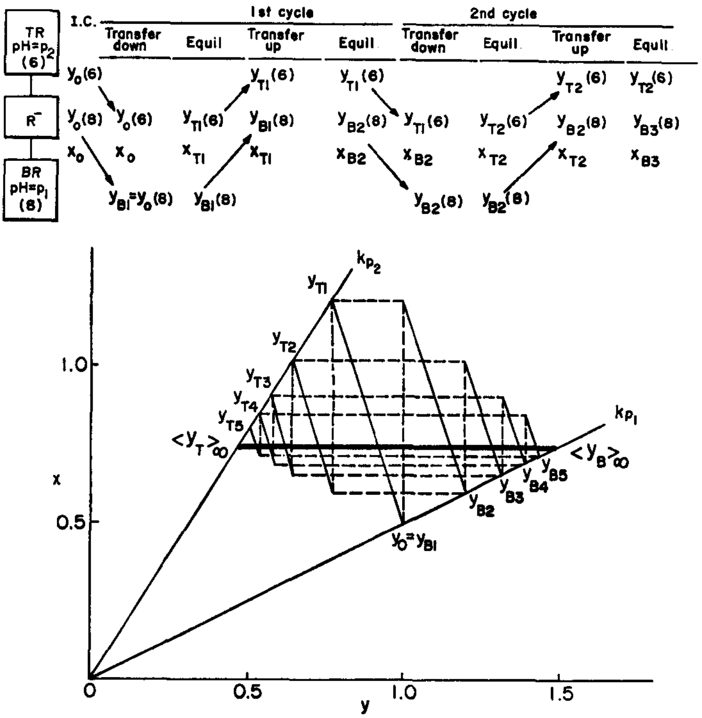

FIG. 4. Graphical solution for a one-column parametric pumping system.

point y_{T1}. The point is located at the intersection of equilibrium line k_{p_2} and of the operating line passing through $(y_0; x_0)$. The slope of the operating line is $(-V/\bar{V})$. (See Eq. 1.)

(c) Transfer up: The solution in column is brought to *TR* and the solution in *BR* is returned to the column. The composition in the column is now $(y_{B1}; x_{T1})$.

(d) Equilibration at P_1: The column pH is shifted back to P_1. The phase equilibrium is reestablished. The new equilibrium point $(y_{B2}; x_{B2})$, represented by the point y_{B2}, is located at the intersection of the equilibrium line k_{p_1} and of the operating line passing through $(y_{B1}; x_{T1})$ and having a slope of $(-V/\bar{V})$. This ends the first cycle.

The second cycle will start from a transfer of the fraction y_{T1} from *TR* to the column and the fraction y_{B2} to *BR*. We then follow the steps described above (see Fig. 4). If the procedure is repeated in each of the succeeding cycles, one can see that as n becomes large, the top and bottom reservoir concentrations will approach steady values, i.e., $\langle y_T \rangle_\infty$ and $\langle y_B \rangle_\infty$, respectively. At steady state the solid phase has a constant composition which is in equilibrium with both $\langle y_T \rangle_\infty$ and $\langle y_B \rangle_\infty$, i.e., $x = k_{p_1}\langle y_B \rangle_\infty = k_{p_2}\langle y_T \rangle_\infty$, and therefore, the line $\overline{\langle y_T \rangle_\infty \langle y_B \rangle_\infty}$ must be parallel to the y axis.

TWO-COLUMN PARAMETRIC PUMPING SYSTEM

The system has two columns and three reservoirs as shown in Fig. 5. One column is packed with a cation exchanger (R^-) and the other with an anion exchanger (R^+). The pH level for the top and bottom reservoirs is maintained at P_1 (= 8) and that for the middle reservoir is kept at P_2 (= 6). Initially, the top reservoir and both columns are filled with a mixture of the concentration y_0. The R^- and R^+ columns are respectively in equilibrium at P_1 (= 8) and P_2 (= 6). One cycle of operation is described as follows:

(a) Transfer down:

Step 1. The fluid in *TR* is transferred to the R^+ column, and the content in the R^+ column goes to *MR* (middle reservoir).
Step 2. The content of the R^- column goes to *BR* and the fluid in *MR* is transferred to the R^- column.

(b) Equilibration: The pH in the R^+ column is changed from P_2 to P_1, and at the same time the pH in the R^- column is shifted from

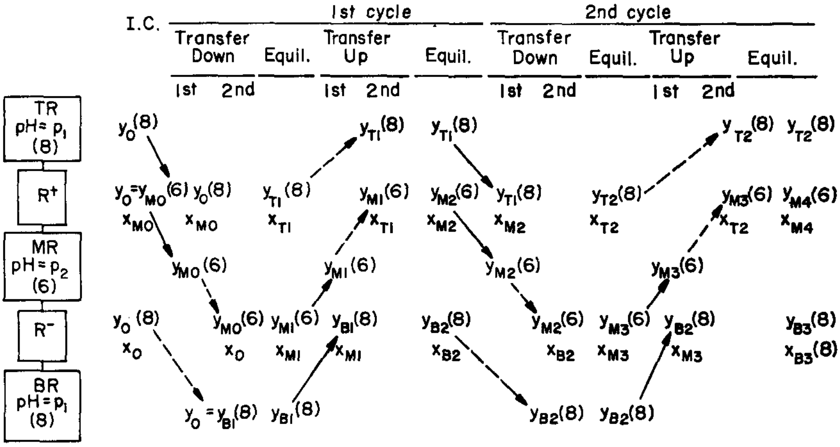

FIG. 5. Description of a two-column parametric pumping system.

P_1 to P_2. Thus reequilibrium is allowed in both columns.

(c) Transfer up: The content in *BR* is brought back to the R^- column. The content in the R^- is pushed through *MR* and goes back to the R^+ column. The content in the R^+ column is transferred to *TR*.

(d) Equilibration: The pH is switched from P_1 to P_2 for the R^+ column, and from P_2 to P_1 for the R^- column. The phase equilibrium is reestablished in both columns. Thus one cycle is completed.

The procedure is repeated for each of the succeeding cycles. The graphical representation is shown in Fig. 6. In this figure there are four equilibrium lines with slopes, respectively, $k_{p_1}{}^-$, $k_{p_2}{}^-$, $k_{p_1}{}^+$, and $k_{p_2}{}^+$. $k_{p_1}{}^-$ and $k_{p_2}{}^-$ are the equilibrium constants of Solute A in the R^- column while $k_{p_1}{}^+$ and $k_{p_2}{}^+$ are for A in the R^+ column. For the purpose of illustration, we assume that $k_{p_2}{}^- = k_{p_1}{}^+$ and $k_{p_1}{}^- = k_{p_2}{}^+$. However, other conditions are conceivable. The graphical construction is similar to that described for the one-column system. From Fig. 6, $\langle y_T \rangle_\infty$, y_{MS} $(= y'_{MS} = y''_{MS})$, and $\langle y_B \rangle_\infty$ are, respectively, the steady-state concentrations for the top, middle, and bottom reservoirs. By connecting the points $\langle y_T \rangle_\infty$, y'_{MS}, y''_{MS}, and $\langle y_B \rangle_\infty$, a two-step staircase is formed. Note that at

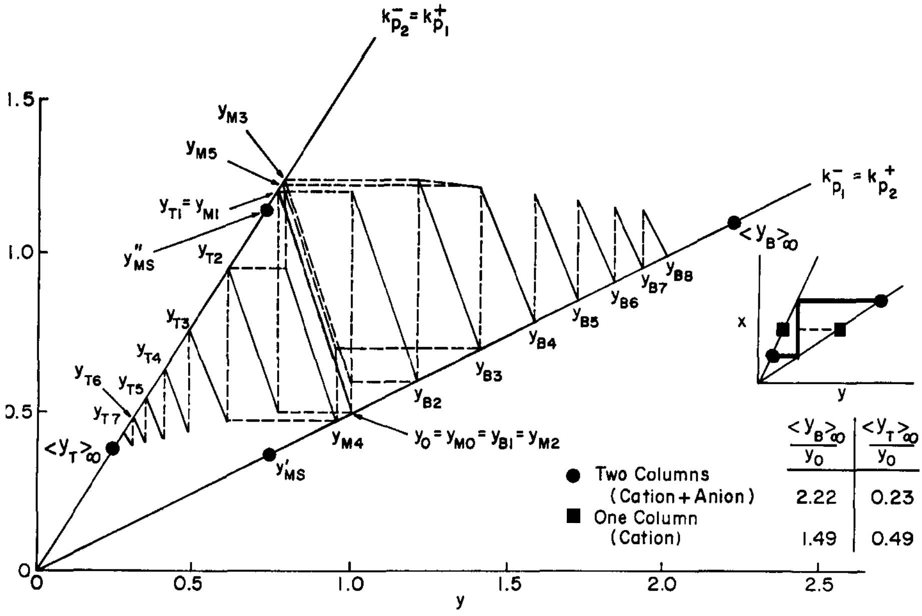

FIG. 6. Graphical solution for a two-column parametric pumping system.

steady state the fraction in the middle reservoir is such that it is in equilibrium with both cation and anion exchangers at pH = P_2, i.e., $y''_{MS} = (x/k_{p_2}{}^-)_{R^-} = y'_{MS} = (x/k_{p_2}{}^+)_{R^+}$.

In the R^+ column the Solute A migrates from the high pH end (pH = 8) toward the low pH end (pH = 6), whereas in the R^- column it moves in the opposite direction. Therefore, we accumulate the Solute A at the high pH end of the R^- column, i.e., the bottom reservoir. If we replot Figs. 4 and 6 to show the separation factor $(\langle y_B \rangle_n / \langle y_T \rangle_n)$ vs n (Fig. 7), one can see that the two-column system is much preferable.

MULTICOLUMN PARAMETRIC PUMPING SYSTEM

The two-column system just described can be extended to the multicolumn system (Fig. 8). The system consists of top and bottom reservoirs and a series of columns and middle reservoirs, i.e., M columns and $(M - 1)$ middle reservoirs (where M = even number). The columns with odd numbers are packed with anion exchangers and the remaining columns are with cation exchangers. pH in both top and bottom reservoirs is

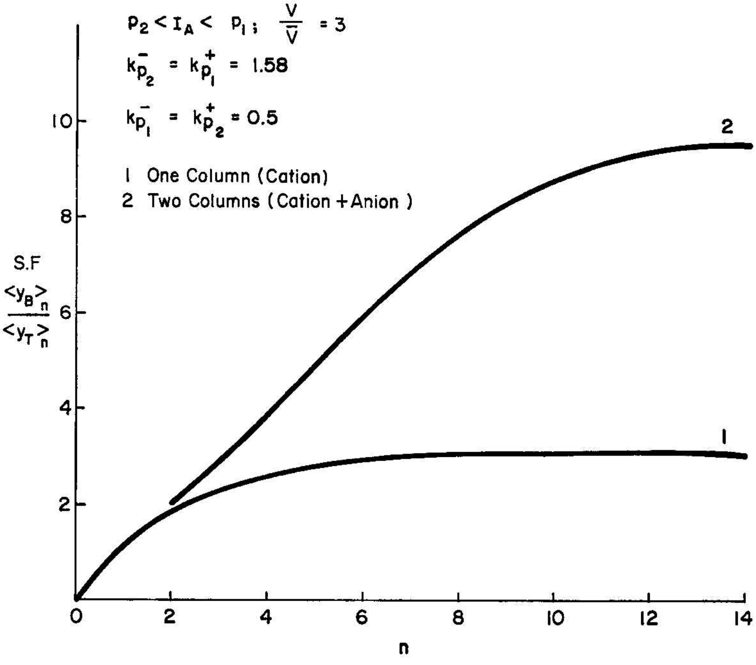

FIG. 7. Separation factors vs n for one- and two-column parametric pumps.

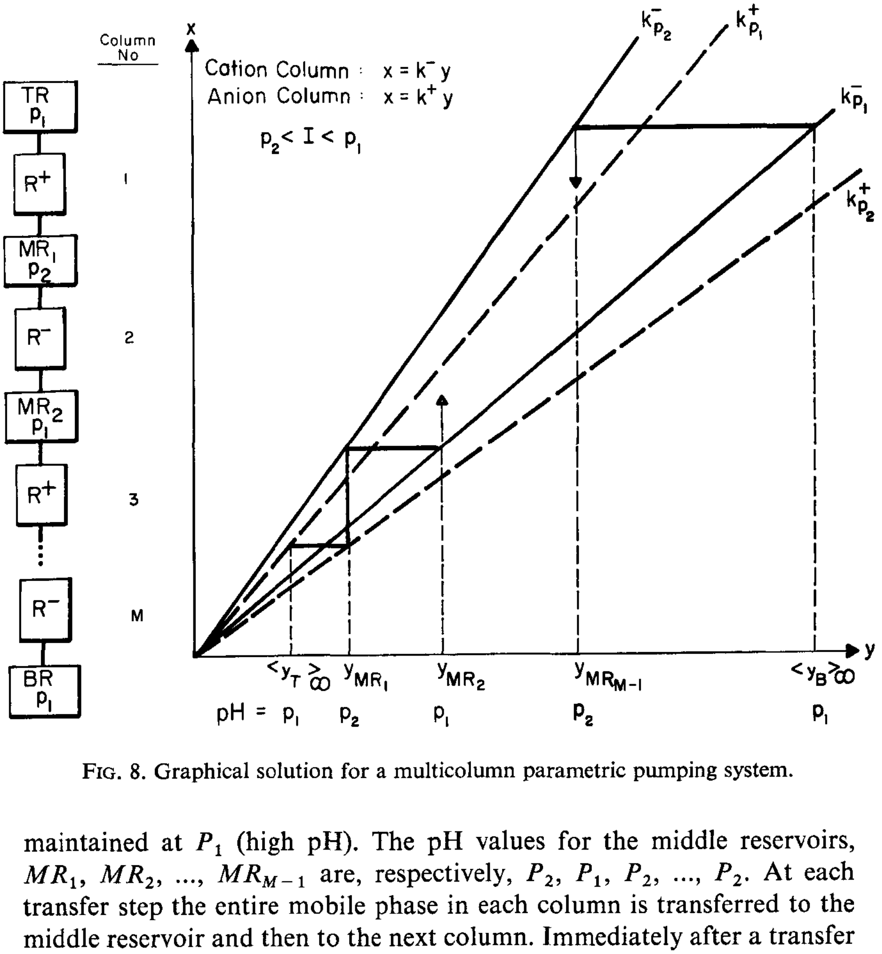

FIG. 8. Graphical solution for a multicolumn parametric pumping system.

maintained at P_1 (high pH). The pH values for the middle reservoirs, MR_1, MR_2, ..., MR_{M-1} are, respectively, P_2, P_1, P_2, ..., P_2. At each transfer step the entire mobile phase in each column is transferred to the middle reservoir and then to the next column. Immediately after a transfer step the two phases in each column are allowed to come to equilibrium. The graphical construction can be made in the same way as described for the one- and two-column parapump systems. After a certain number of cycles the construction converges toward a limit, represented by an M-step staircase between $k_{p_1}{}^+$, $k_{p_1}{}^-$, $k_{p_2}{}^+$, and $k_{p_2}{}^-$. A very high separation factor $(\langle y_B \rangle_\infty / \langle y_T \rangle_\infty)$ can be obtained when M becomes large. Figure 9 shows the dependence of the steady-state separation factor $(\langle y_B \rangle_\infty / \langle y_T \rangle_\infty)$ on M. As M increases, $(\langle y_B \rangle_\infty / \langle y_T \rangle_\infty)$ increases without limit. Note that the results are based on the equilibrium theory, which provides the upper limit of separation of the process.

The picture of batch parametric pump operations developed in the

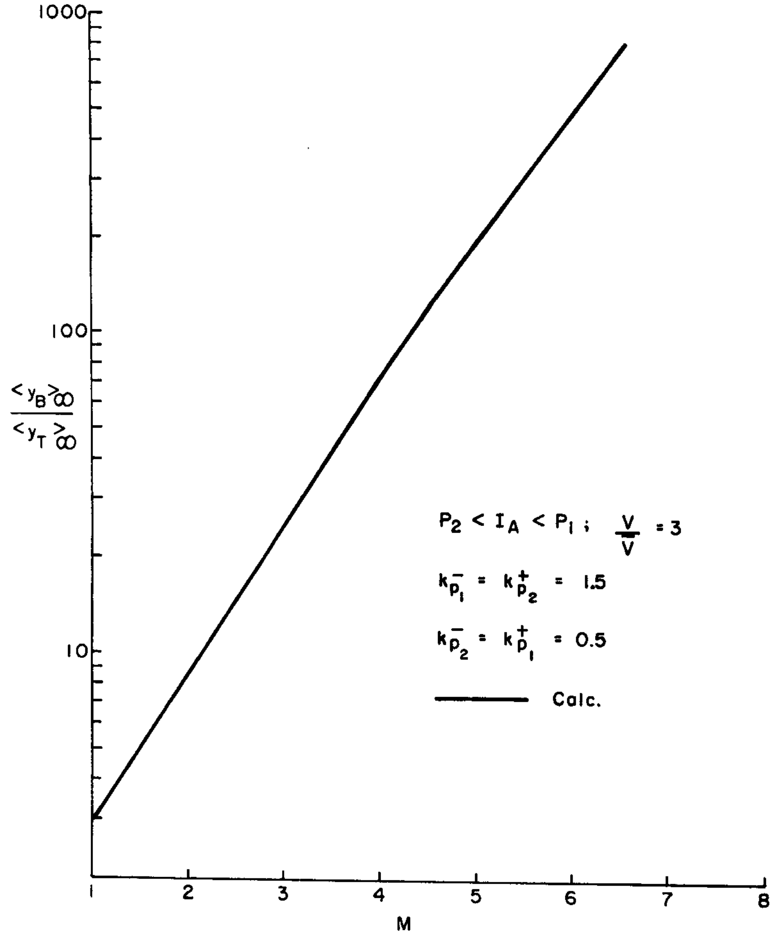

FIG. 9. Steady-state separation factors vs number of columns.

present paper can also be extended to continuous parapump systems and will be presented in subsequent papers.

EXPERIMENTAL DATA

The experimental apparatus was similar to that used previously (*1*, *2*). The systems selected to be examined experimentally were haemoglobin–buffer and albumin–buffer. The isoelectric points for haemoglobin and albumin are 6.7 and 4.7, respectively. The ion exchangers used were CM-

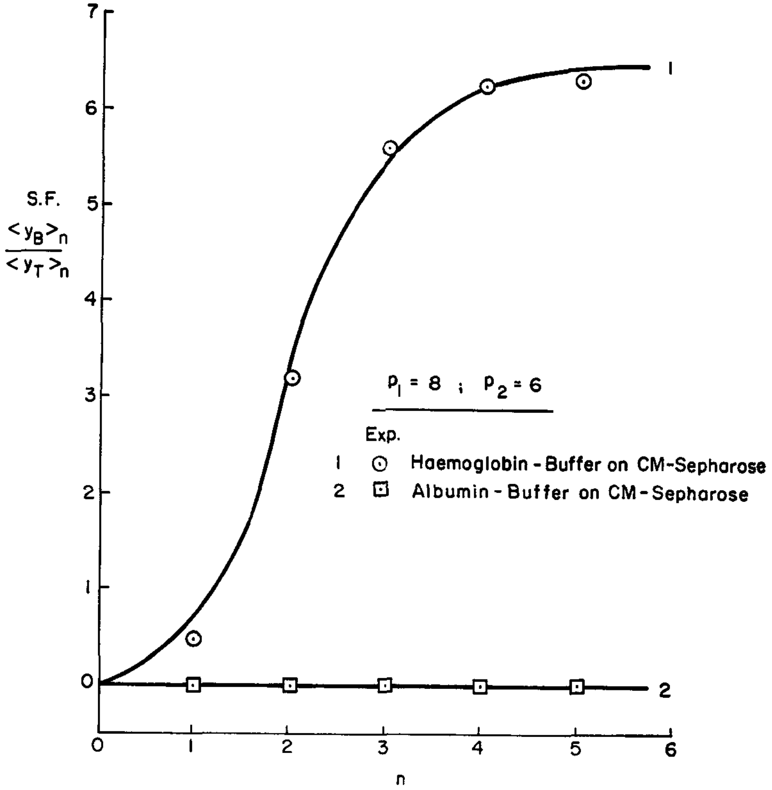

FIG. 10. Experimental results for one-column parametric pump.

Sepharose (cation, R^-) and DEAE-Sepharose (anion, R^+) manufactured by Pharmacia Fine Chemicals. The results are shown in Figs. 10 and 11. For all runs α was set approximately equal to 1, and the reservoir displacement was 0.017 cm^3/sec.

Figure 10 illustrates the separation factor $(\langle y_B \rangle_n / \langle y_T \rangle_n)$ vs n for a one-column parametric pump. Initially, the feed solution containing a solute (haemoglobin or albumin) was present in the top reservoirs only. The column and the bottom reservoir dead volume were filled with the buffer solution of pH = 8. The buffer solutions were made from monobasic and dibasic sodium phosphate. The top and bottom reservoirs were maintained at pH = 6 (P_2) and pH = 8 (P_1), respectively, so that the isoelectric point of haemoglobin would lie between the two pH levels. As a result of a change in the column pH, haemoglobin experiences a change in the net charge and migrates toward the high pH end or the bottom reservoir. Thus

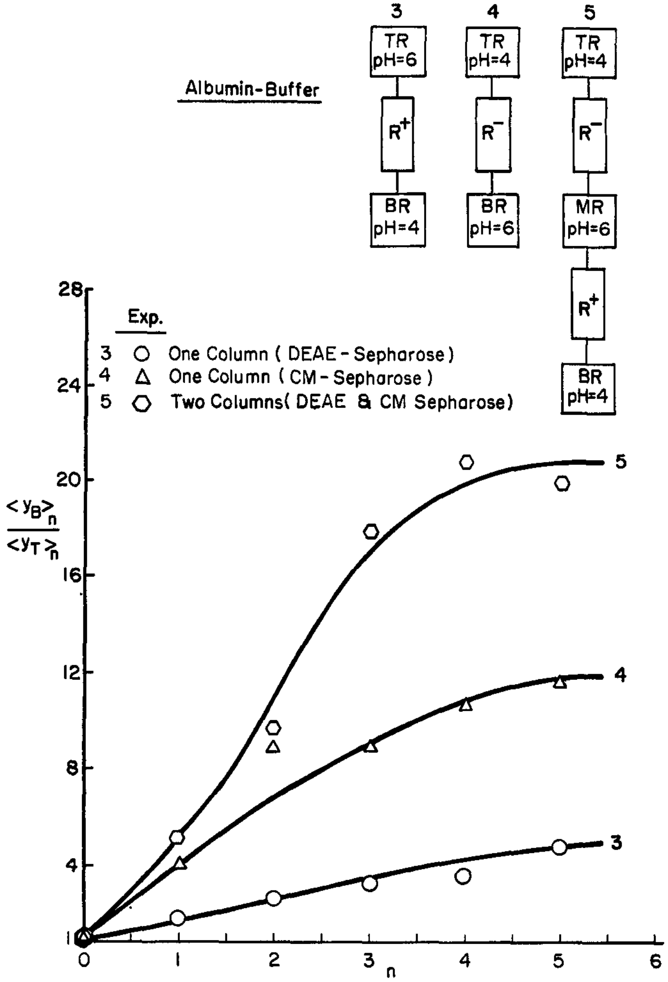

FIG. 11. Comparison of experimental results between one- and two-column parametric pumps.

the separation factor (SF) for hemoglobin increases with *n* and approaches a limiting value. For the case of albumin, $I_{\text{albumin}} = 4.7 < P_2$, and the net charge is always negative during upflow and downflow. As a result, the albumin concentration is unaffected by the parametric pumping operation and remains at zero.

Figure 11 shows the comparison of one- and two-column parapumps. For all cases (Runs 3, 4, and 5) the solute (albumin) was present in the columns and reservoirs in concentration y_0 initially. Two pH levels, 4 and 6, were chosen to bracket the isoelectric point of albumin. The buffers used for this part of the experiments were mixtures of acetic acid, sodium acetate, and sodium chloride. As the theory predicts, albumin is concentrated at the low pH end of the R^+ column (Run 3) and at the high pH end of the R^- column (Run 4). Also, the two-column parapump has much higher separating capability than the one-column unit.

CONCLUSIONS

The performance of pH parametric pumps is analyzed in terms of an equilibrium theory. We have examined one-, two-, and multicolumn parapump systems, and shown by graphical construction on the equilibrium diagram how the separation builds up from cycle to cycle. The results indicate that parametric pumping can be quite effective if a system consisting of a series of columns packed alternately with cation and anion exchangers is chosen.

The separation capability of one- and two-column parapumping is demonstrated experimentally for the systems of haemoglobin–buffer-CM Sepharose, albumin–buffer–CM Sepharose, and albumin–buffer–CM Sepharose–DEAE Sepharose. A separation factor greater than 20 has been obtained. Observed values are in qualitative agreement with the parapump theory.

SYMBOLS

I	stage number
I_i	isoelectric point of i
IS_1	ionic strength in the bottom reservoir
IS_2	ionic strength in the top reservoir
J	transfer step
k	x/y, equilibrium constant
k_{p_1}	equilibrium constant at pH $= P_1$
k_{p_2}	equilibrium constant at pH $= P_2$
n	number of cycles of pump operation
M	number of columns
N	number of stages or cells
P_1	high pH level
P_2	low pH level
Q	reservoir displacement rate, cm^3/sec
V	volume of fluid phase per stage, cm^3
$\bar{V}$	volume of solid phase per stage, cm^3

V_B	bottom reservoir dead volume, cm^3
V_{MR}	middle reservoir dead volume, cm^3
V_T	top reservoir dead volume, cm^3
x	concentration of solute in the solid phase, kg mole/cm^3
y	concentration of solute in the fluid phase, kg mole/cm^3
y_0	concentration of solute in the feed, kg mole/cm^3
$\langle y_B \rangle_n$	average concentration of solute in the bottom reservoir at *n*th cycle, kg mole/cm^3
$\langle y_T \rangle_n$	average concentration of solute in the top reservoir at *n*th cycle, kg mole/cm^3
$\langle y_B \rangle_\infty$	steady-state concentration of solute in the bottom reservoir, kg mole/cm^3
$\langle y_T \rangle_\infty$	steady-state concentration of solute in the top reservoir, kg mole/cm^3
α	(reservoir displacement)/(column void volume)
π/ω	duration of upflow or downflow

Acknowledgment

The National Science Foundation (CPE 77–04129 and CPE 79–10540) provided financial support for this research.

REFERENCES

1. H. T. Chen, T. K. Hsieh, H. C. Lee, and F. B. Hill, *AIChE J.*, *23*, 695 (1977).
2. H. T. Chen, Y. W. Wong, and S. Wu., *Ibid.*, *25*, 320 (1979).
3. G. Grevillot and D. Tondeur, *Ibid.*, *22*, 1055 (1976).
4. T. J. Jenczewski and A. L. Meyers, *Ind. Eng. Chem., Fundam.*, *9*, 216 (1970).
5. R. L. Pigford, B. Baker, and D. E. Blum, *Ibid.*, *8*, 144 (1969).
6. J. E. Sabadell and N. H. Sweed, *Sep. Sci.*, *5*, 171 (1970).
7. A. G. Shaffer and C. E. Hamrin, *AIChE J.*, *21*, 782 (1975).

Received by editor November 5, 1979